

# Computer Simulations of Natural and Synthetic Polymers in Confined Systems

S. Piotto,<sup>\*1,2</sup> S. Concilio,<sup>1,2</sup> F. Mavelli,<sup>3</sup> P. Iannelli<sup>1,2</sup>

**Summary:** Nanotechnology is the ability to work at the molecular and supramolecular levels in order to create and use devices, structures and systems with the desired properties and functions. This is what Nature already does in living systems. In this work we investigated the consequences of confinement in the ordering of natural (namely proteins) and synthetic polymers by means of computational techniques. The focus is put on the possibility to design new materials in a Nature-like fashion. In the first part of the paper, the possibility to select/design different folding of the same peptide is investigated by means of full atoms molecular dynamics. In the second part of the paper dynamic mean-field density functional method is applied to the dynamics of block copolymer melts in three-dimensional lattice model. The analysis of the aggregates and their temporal evolution in free space and in confined space are compared.

## Introduction

Nanotechnology is the ability to have a control of matter on atomic, molecular and supramolecular levels (on a scale of 1–100 nm), in order to create and use devices, structures and systems with the desired properties and functions emerging from their nanoscopic sizes. If the goal of nanotechnology is to hierarchically assemble molecules into objects, along several length scales, and to disassemble objects into molecules, then Nature is truly a brilliant nano engineer having been so for billions of years. There is an abundance of ‘smart’ biological materials with hierarchical nanostructures - built from proteins - that are capable of adapting to new tasks, are self-healing, and can simply self-assemble out of a solution of building blocks. An obvious, as well as ancient, goal is to learn

from Nature the techniques to obtain an aggregate with the desired properties.<sup>[1]</sup>

Unfortunately, how proteins fold into a unique native structure remains an important unanswered question. There have been many *in vitro* and *in silico* experiments that have provided insights into the folding mechanism<sup>[2,3]</sup> but most of these studies were focused on dynamics of proteins in infinite dilution. *In vivo* proteins exhibit their dynamic behavior in a crowded cellular environment and/or in confined spaces such as the chaperonin cavity, the proteosome, the ribosome exit tunnel, etc. When considering these factors, it is reasonable to assume that proteins may experience different energy landscapes when they fold *in vivo* context rather than in solution bulk, and these differences may constitute a significant piece of the folding puzzle. In previous works,<sup>[4,5]</sup> confinements have been treated both analytically and via simulation using polymer physics models. These models predict that confinement reduces the conformational entropy of the unfolded state ensemble, by excluding the more extended structures, and this leads to the relative stabilization of the folded

<sup>1</sup> Department of Pharmaceutical Sciences, University of Salerno, Italy  
E-mail: piotto@unisa.it

<sup>2</sup> Research Centre for Nanomaterials and nanotechnology NANOMATES, University of Salerno, Italy

<sup>3</sup> Department of Chemistry, University of Bari, Italy

state. A close look into protein folding shows that spontaneous non-assisted folding occurs only for small proteins. Many proteins fold or are refolded with the assistance of chaperons and chaperonins, which are also proteic structures capable of binding to a broad range of proteins. It was suggested that confinement into the chaperonin cage itself can significantly accelerate folding of a substrate.

Since proteins are block polyamides made up of 20 different building blocks, we can try to apply what we learned from Nature to different synthetic polymers.

A substrate protein is remarkably stabilized by confinement; the increase in denaturation  $\Delta T_f$  was estimated by Takada as large as 60 °C.<sup>[6]</sup> For a protein of size  $R_0$  inserted in a cylinder of radius  $L$  and length  $2L$ , the stabilization  $\Delta T_f$  scales as  $(R_0/L)^v$ , where  $v \sim 3$ , which is consistent with a mean field theory of polymer.<sup>[6]</sup>

The confinement of a protein has a significant energy cost, which increases with  $R_0/L$ , indicating that the confinement requires external work that can be provided by the chaperonin system. About kinetics, the same study shows that folding is accelerated in confined case. This finding is consistent with the experimental result of encapsulated proteins in silica matrix.<sup>[7]</sup> This stabilization is surprisingly large when the size of the substrate protein is comparable to the cage scale. There are at least three different, but not mutually exclusive, scenarios.<sup>[5]</sup> The first “Anfinsen cage” model indicates that the chaperonin provides a passive cage that separates a substrate protein from other macromolecules, limiting the possibility of aggregation.<sup>[8]</sup>

In the other “iterative annealing” scenario, a substrate protein is mechanically forced to unfold upon binding to chaperonin and it folds upon transfer into the cavity or release from it. This cycle is repeated until a substrate reaches the native state. Both Anfinsen cage and mechanical unfolding effects may be present in reality.

Using an engineered chaperonin system that inhibits the chaperonin cycle, Brinker

et al.<sup>[9]</sup> showed that confinement of unfolded protein alone accelerates folding inside the cage.

Zhou and Dill formulated an elegant analytical model to explain this effect.<sup>[10]</sup> They modeled a chaperonin as an inert sphere of a given radius, and they treated the unfolded state as a Gaussian chain. They solved a classical diffusion equation under spherical boundary conditions. Using this solution, they predicted the  $\Delta\Delta G$  (change in free energy of folding) for confinement of a protein of a certain length confined to a cavity of fixed size. This model predicts that a large stabilization of the folded state is expected to occur when the size of the confining volume is only slightly larger than the native state. Beyond this, the native state will not fit inside the cavity and the free energy goes to infinity. As the confining volume increases, the confinement-induced stabilization approaches zero. The confinement influences also the assembly of a polymer melt. For diblock copolymer melt that exhibits a lamellar morphology in the bulk, it has been observed that when placing these copolymers between hard, flat surfaces, the distance between the surfaces must be commensurate with the natural lamella period, otherwise deviation from natural periodicity occurs, which forces a change from the bulk equilibrium morphology.<sup>[11,12]</sup> The effect of confinement on diblock copolymers has been explored by Russell and co-workers. They reported the study of symmetric and asymmetric polystyrene-*b*-polybutadiene (PS-*b*-PBD) diblock copolymers<sup>[13]</sup> confined within nanoscopic cylindrical pores in alumina membranes. Theoretically, concentric cylinder structures have been predicted by He et al.<sup>[14]</sup> using Monte Carlo simulations and by Sevink et al.<sup>[15]</sup> using dynamical density functional simulations. Furthermore, Wickham et al.<sup>[16]</sup> have carried out self-consistent field theory (SCFT) calculations for diblock copolymers under cylindrical confinement, and concentric cylindrical structures were obtained among other two-dimensional morphologies.

Recently Shi et al.<sup>[17]</sup> reported a study of symmetric diblock copolymers confined in spherical nanopores by means of simulated annealing Monte Carlo simulations.

To the best of our knowledge, all the previous work concentrate on the stabilization of the folded state, or to the kinetics of the folding. In the following, we will try to consider confinement for stabilizing native state as well as selecting a different state. These observations clearly disclose the possibility to design new materials.

## Methods

### Molecular Dynamics Simulations

The simulations have been performed with the NAMD<sup>[18]</sup> package on clusters of 8 processors. The visualization is provided by the program VMD.<sup>[19]</sup> Partial charges are calculated using the semi-empirical methods PM3. The target molecules are modeled using the CHARMM force field parameters.

Peptides and water molecules were separately coupled to a heat bath at temperature  $T = 310$  K using the Langevin thermostat with a coupling time constant of 0.1 ps. For simulations in spherical cage, we have employed a spherical shell with a diameter of 30 nm made of constrained waters. A very simple peptide has been chosen: the peptide  $V_{10}S_{10}V_{10}S_{10}V_{10}$  is made of 50 aminoacids, 20 polars and 30 apolars. The peptide has been scaled down to be inserted in the cage and then the molecules are let relax the bonding energy.

Pressure was controlled using the Langevin barostat with a time constant of 1 ps. Lennard-Jones interactions were set at a distance of 1.0 nm and the time step set to 1 fs. The systems were simulated for a total of 10–50 ns each. This permitted system equilibration and the subsequent data collection.

### Dynamic Density Functional Theory Simulations

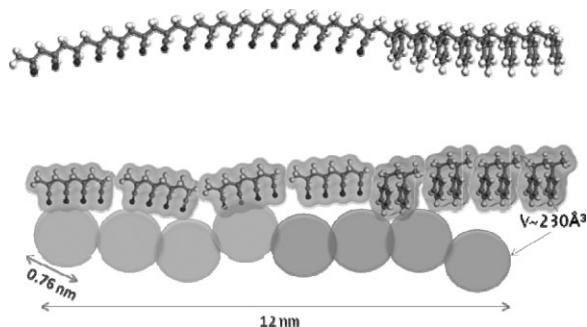
MesoDyn<sup>[20]</sup> is an important mesoscopic simulation technique, which is based on

dynamic mean field density functional theory (DDFT). An important advantage of MesoDyn is the time integration of functional Langevin equations.

The basic idea in the MesoDyn method is the density functional theory. It is based on the idea that the free energy  $G$  of an inhomogeneous liquid is a function of the local density function  $G$ . From the free energy, all thermodynamic functions can be derived. The model used in the MesoDyn project consists of beads of various types  $i, j, \dots$  with interactions described by harmonic oscillator potentials for the intramolecular interactions (Gaussian chain) and a mean field potential for all other interactions. Detailed theories on MesoDyn are introduced in the literatures.<sup>[21,22]</sup> The dynamics of the system is described by a set of functional Langevin equations. They represent diffusion equations in the component densities, which take account of the noise in the system. Each bead represents a group of atoms corresponding to a structural units of a polymer chain. The chain topology depends on the degree of coarsening of the original system.

A PAN-*b*-PS diblock copolymer is a polymer consisting of a sequence of polyacrylonitrile-type monomers chemically joined to a sequence of polystyrene-type monomers. Phase transitions in PAN/PS mixture can be induced even by a small amount of incompatibility, i.e. a different affinity between PAN and PS monomers. However, when PAN-homopolymer and PS-homopolymer are chemically joined in a diblock copolymer a macroscopic phase separation is not observed. Instead a number of order-disorder phase transitions take place in the system among the isotropic phase and spatially ordered phases where PAN and PS rich domains are periodically arranged. The covalent bond joining the two blocks rests at the interface between PAN and PS domains. We have chosen this system that is well known, completely characterized and easy to process.

The copolymer is modeled by two spherical beads, PS representing 2 units of

**Figure 1.**

Representation of a portion of PAN-*b*-PS block copolymer and its reduction to beads.

polystyrene, and PAN representing 6 units of polyacrylonitrile, with a volume of  $230 \text{ \AA}^3$  (Figure 1). The topology of the copolymer is linear and of type  $\text{PAN}_i\text{-PS}_j$  with  $i$  and  $j$  indicating the number of beads in the chain.

All the mesoscale simulations and analyses were done with the MesoDyn module in Materials Studio 4.0.<sup>[20]</sup> The dimensions of the cage was set in the range of  $20 \div 100 \text{ nm}$ . To ensure a stable numerical algorithm, as an approximation, all bead diffusion coefficients were  $1.0 \cdot 10^{-7} \text{ cm}^2 \text{ s}^{-1}$ . The simulation temperature was  $298 \text{ K}$ , the time step was  $50.0 \text{ ns}$  and the noise-scaling parameter was 100. The mean-field interaction energy ( $a_{ij}$ ) between different chemical components is related to the Flory–Huggins interaction parameter through the equation:

$$v^{-1} \varepsilon_{ij} = \chi_{ij} RT \quad (1)$$

where  $v^{-1} \varepsilon_{ij}$  is the input parameter.

The approximate values for the MesoDyn interaction parameters between various beads are given in Table 1.

## Results and Discussion

### Peptides

The inner wall of the chaperonin chamber is known to be largely hydrophilic, and thus it is unlikely that substrate proteins strongly interact with inner wall atoms via hydrophobic interactions. In order to simulate the principle mechanism of confinement assisted folding, we employed a spherical mask made of water molecules with fixed position. Physically, a polymer confined into a small volume exhibits characteristic behavior caused by change in its conformational entropy. We performed several simulations changing peptide and cage diameter. For the peptide  $\text{V}_{10}\text{S}_{10}\text{V}_{10}\text{S}_{10}\text{V}_{10}$  we have carried out a simulation in vacuum, in water, in a polar cage filled with water,

**Table 1.**

Some relevant parameters of the PS and PAN portion.

Monomer	Repeat unit length	van der Waals volume	Glass transition temperature Tg	Solubility parameter	Surface tension	Dielectric constant at 298K
PS	5.094	128.077	381.67	19.515	45.949	2.567
PAN	10.184	129.420	362.52	24.554	61.145	3.991

Energies	Chi (298 K)	Emix (298 K)	Repulsion parameter
PS-PAN	122.07	72.29	4.75

and in a more complex cage made of hydrophilic and hydrophobic parts filled with water. The initial geometry was  $\alpha$ -helix and was kept identical in the four simulations. The peptide folds out in very different structures. Comparison between free folding and cage assisted folding confirms the observation that the folding is much faster in confined space.

Comparison between MD calculations with and without (not shown) confinement show important differences. First of all, due to the limitation of conformational motion, the peptide in cages converge into a stable structure in few nanoseconds. These times are order of magnitude shorter than the ones observed in bulk. It is important to observe that there are differences also among different types of confinement. Figure 2 shows the different final conformations achieved by the same peptide  $V_{10}S_{10}V_{10}S_{10}V_{10}$  in a spherical cage with and without an apolar region of diameter approximately one third of the diameter of the sphere. The presence of this region profoundly alters the thermodynamics and the kinetics of the peptide

and the final conformations. In Figure 3 the root mean square deviation (RMSD) of the peptide in case of polar spherical confinement (Figure 2a) and in case of polar-apolar spherical caging (Figure 2c) indicates that the presence of a hydrophobic region furthermore restricts the mobility of the peptide. The RMSD calculated for the whole peptide during the entire dynamic, increase from  $\approx 0.18 \text{ \AA}$  in the case of pure polar cage, to  $\approx 0.22 \text{ \AA}$  in case of polar-apolar cage.

### Polymers

We study the ordering dynamics of polymer organization using a mesoscopic simulation technique, which is based on dynamic mean field density functional theory. The polymers are confined to small spherical nanodomains. The effect of caging on polymers can be explained by the restriction on the local chain direction near the domain surface in the crystal nucleation stage and the restriction of large orientation relaxation and coalescence in the crystal growth stage. Simulation results reveal that

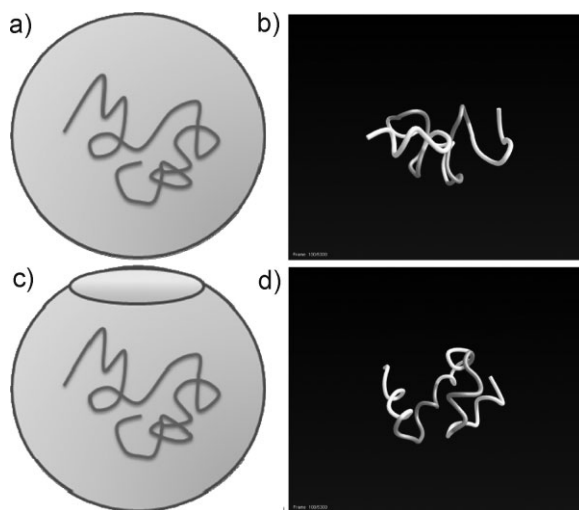


**Figure 2.**

The peptide used in the MD simulation is inserted in the spherical cage after resizing. The sphere represented in (a) is a symmetric and polar confinement. In (b) is represented the equilibrium after 2 ns of simulations. The sphere represented in (c) presents an apolar region made up constrained methane molecules. The presence of this apolar region has a drastic effect in the final conformation (d). In (b) and (d) the water molecules and the cage are not represented for clarity. The peptide is shown as tube in white (valine) and light grey (serine).

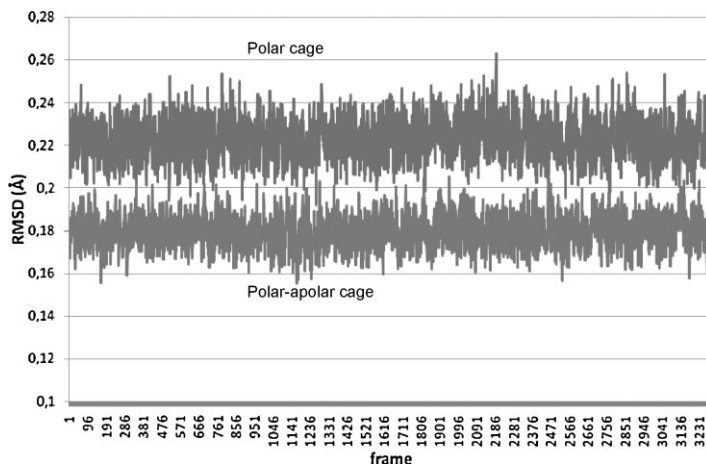


**Figure 3.**

Time evolution of RMSD for polar and semipolar (polar-apolar) spherical confinement.

the confinement by the noncrystalline medium does not simply have an effect on the polymer crystallization dynamics, but has various combined effects depending on the time stage, the rigidity of polymer chains, and the strength of the surrounding domain interface.

PAN-*b*-PS system, when let evolve without constriction under periodic boundary conditions (PBC), rapidly reach a lamellar organization. In our systems we observe the formation of stable lamellae for time longer than 500  $\mu$ s (Figure 4).

In order to obtain the confinement of PAN-*b*-PS system, we have generated repulsive mask of different size and shape.

Initially we used a spherical mask and we kept the composition of the system constant. We have run an extended set of calculations in which we varied the diameter of the sphere or the length of the polymer chains (the latter case is not shown).

The case of spherical confinement at 20 nm is particularly simple (Figure 5). Since the confinement does not permit the polymers to self organize in lamellae, the system spontaneously adopts a conformation in which the PS inner layer is saddle-like shaped. The reason for this conformation is obvious if one recall that the bending elasticity is the most important energy

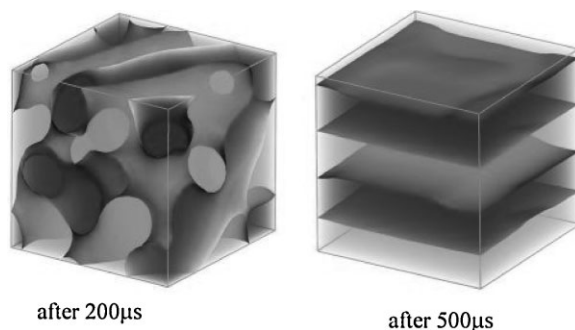


**Figure 4.**

Time evolution of PAN-*b*-PS system. The boundary between PAN and PS regions is represented with isosurfaces. In dark grey is represented PS.



**Figure 5.**

PAN-*b*-PS system inside a sphere of diameter equal to 20 nm. The boundary between PAN and PS regions is represented with isosurfaces. In dark grey is represented PS, in light grey PAN.

terms for fluid surfaces. It can be described by the famous Helfrich Hamiltonian (2):

$$g = \frac{1}{2} \kappa (c_1 + c_2 - c_0)^2 + \kappa_G c_1 c_2$$

$$= 2\kappa (H - 2c_0)^2 + \kappa_G K \quad (2)$$

where  $c_1, c_2$  are the principal curvatures while  $H$  is the mean and  $K$  the Gaussian curvature and  $c_0$  is the spontaneous curvature.  $\kappa$  and  $\kappa_G$  are the bending rigidity and the Gaussian bending rigidity, respectively. In this saddle configuration the mean curvature  $H$  (which is the average of the principal component of the curvature) is zero everywhere, whereas the Gaussian curvature  $K$  is negative. Consequently, with  $H=0$  the first term of the Hamiltonian vanishes and second is a topological invariant in virtue of the Gauss-Bonnet theorem.

For higher values of the cage diameters, many other variations of the Helfrich's geometries appear. In all cases, the morphologies obeys to the rules of keeping the mean curvature close to zero and reducing the exposition of the edges. An interesting example is given by droplets with diameters of 60 to 150 nm. The morphologies, close to other nanoflowers systems,<sup>[23]</sup> have very interesting features. A radial distribution of lamellae is easily

recognizable when only one block is visualized. This kind of “petals” irradiate from the inner core where they have to cope with a complex topological problem. In fact, while the petals have zero mean curvature, the centre could have a much higher curvature, and consequently it could be energetically costly. It turns out that the center of the nanosphere has the structure of a minimal surface, which is, by definition, a zero curvature surface.<sup>[24]</sup> Minimal surfaces have many interesting applications, ranging from photonic crystals to drug delivery systems. Experimentally, this structured nanospheres can be easily realized via spray pyrolysis. In Figure 8 some TEM images of spheres of PAN-*b*-PS system are shown for comparison with simulations.<sup>[25]</sup> It is noteworthy to notice that a bicontinuous inner core has a tremendous effect in the diffusion of drug out of the particle. This observation could have some consequences in designing novel drug delivery systems.

## Conclusion

From our MD simulations, we have seen that the presence of a cage can assist folding of proteins in a nonspecific manner, and

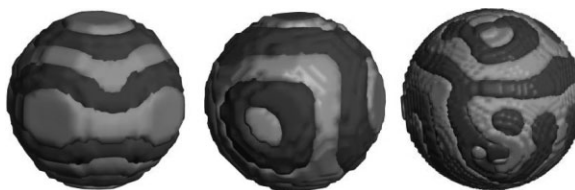


**Figure 6.**

PAN-*b*-PS system inside a sphere of diameter equal to 40 nm. The boundary between PAN and PS regions is represented with isosurfaces. In dark grey is represented PS, in light grey PAN.



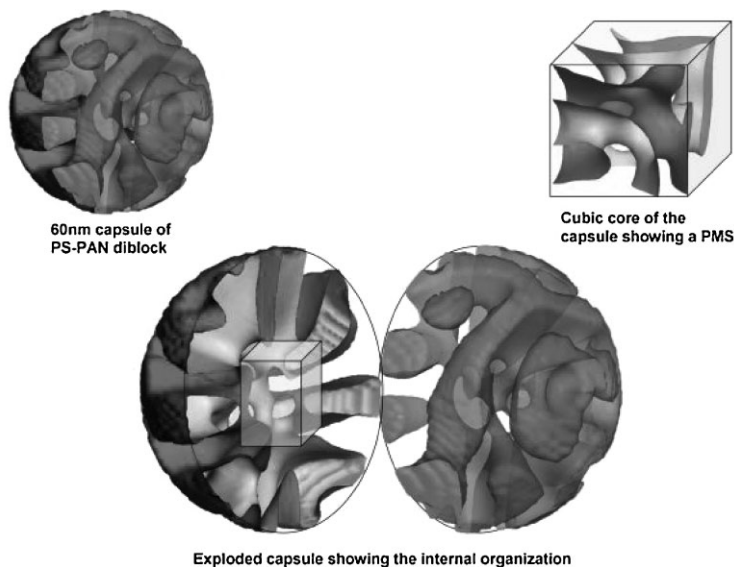


**Figure 7.**

PAN-*b*-PS system inside a sphere of diameter equal to 60 nm. The boundary between PAN and PS regions is represented with isosurfaces. Only PS is represented. Top left image represents the external side of the sphere. Top right image is the detail of the centre of the sphere. Bottom picture shows the sphere cut apart and the core of the sphere evidenced in the box.

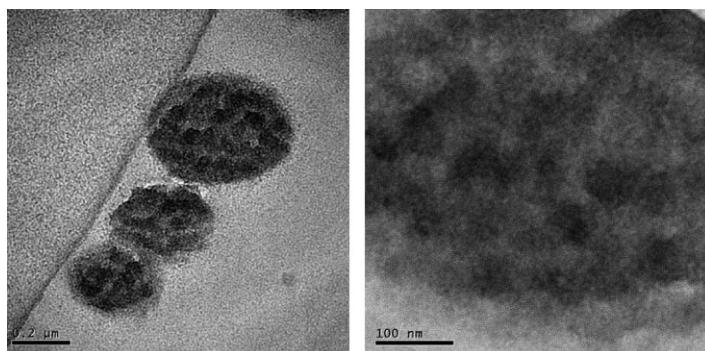


**Figure 8.**

TEM images of nanospheres of PAN-*b*-PS system cutted and shadowed with RuO<sub>4</sub>, revealing the inner organization (images kindly given by Massimo Lazzari, University of Santiago de Compostela, Spain.)

thus any specific interaction between the substrate and the inner wall is not crucial. A primary effect of caging may be to restrict conformational motion of a protein into a small volume. We emphasize that this caging effect must exist on top of any other factors assisting protein folding. To the best of our knowledge, all the previous work concentrated on the stabilization of the

folded state, or to the kinetics of the folding. We have demonstrated that caging not simply, or not only, stabilize the native state of a protein, but in most cases select a different state. Confined systems offer several advantages over systems without any spatial restriction. Since the conformational motions are highly reduced, the folding and the self-assembly occur much



faster. Consequently, since the systems reach an equilibrium within microseconds, small systems become accessible to molecular dynamics investigations, and larger systems (up to 10  $\mu\text{m}$ ) can be treated with DDFT. The possibility to simulate polymer aggregates in details disclose the opportunity to design and produce novel nanomaterials. Once the lesson of Nature is, even roughly, understood the possibility to control folding will not be limited to natural proteins, (i.e. polyamides), but it can be applied to any sort of polymers better suited for modern applications, from optics to electronics, from lubricants to smart delivery systems.

- [1] M. Lazzari, M. A. Lopez-Quintela, *Advanced Materials*. **2003**, 19, 1583–1594.
- [2] A. Fersht, V. Dagget, *Cell*, **2002**, 108, 573–582.
- [3] C. D. Snow, et al. How well can simulation predict protein folding kinetics and thermodynamics? *Annu. Rev. Biophys. Biomol. Struct.* **2005**, 34, 43–69.
- [4] H. Zhou, Protein folding in confined and crowded environments. *ScienceDirect*, **2008**, 469, 76–82.
- [5] D. Thirumalai, D. K. Klimov, G. H. Lorimer, Caging helps proteins fold. *PNAS*, **2003**, 100(20), 11197.
- [6] F. Takagi, N. Koga, S. Takada, How protein thermodynamics and folding mechanisms are altered by the chaperonin cage: Molecular simulations. *PNAS*, **2003**, 100(20), 11367–11372.
- [7] D. K. Eggers, J. S. Valente, *Protein Sci.* **2001**, 10, 250–261.
- [8] F. Weber, F. Keppel, C. Georgopoulos, M. K. Hayer-Hartl, F. U. Hartl, *Nat. Struct. Biol.* **1998**, 5, 977–985.
- [9] A. Brinker, et al. *Cell*. **2001**, 107, 223–233.
- [10] H. Zhou, K. A. Dill, Stabilization of proteins in confined spaces. *Biochemistry* **2001**, 40, 11289–11293.
- [11] P. Lambooy, et al. Observed frustration in confined block copolymers. *Phys Rev Lett* **1994**, 72(18), 2899–2902.
- [12] S. P. Gido, E. L. Thomas, *Macromolecules*. **1994**, 27, 849.
- [13] K. S. Xiang Hongqi, Taehyung Kim, Sungin Moon, T. J. McCarthy, T. P. Russell, The influence of confinement and curvature on the morphology of block copolymers. *Journal of Polymer Science Part B: Polymer Physics*, **2005**, 43(23), 3377–3383.
- [14] X. He, et al. Self-assembly of the symmetric diblock copolymer in a confined state: Monte Carlo simulation. *The Journal of Chemical Physics* **2001**, 114(23), 10510–10513.
- [15] G. J. Sevink, A. V. Zvelindovsky, Block copolymers confined in a nanopore: pathfinding in a curving and frustrating flatland. *J Chem Phys* **2008**, 128(8), 084901.
- [16] W. Li, R. A. Wickham, R. A. Garbary, Phase Diagram for a Diblock Copolymer Melt under Cylindrical Confinement. *Macromolecules* **2006**, 39(2), 806–811.
- [17] B. Yu, et al. Self-Assembly of Symmetric Diblock Copolymers Confined in Spherical Nanopores. *Macromolecules* **2007**, 40(25), 9133–9142.
- [18] J. C. Phillips, et al. Scalable molecular dynamics with NAMD. *J. Comp. Chem.* **2005**, 26, 1781–1802.
- [19] W. Humphrey, A. Dalke, K. Schulten, VMD - Visual Molecular Dynamics. *J. Molec. Graphics* **1996**, 14, 33–38.
- [20] I. Accelrys, *Materials Studio 4.0*.
- [21] S. S. Jawalkar, T. M. Aminabhavi, Molecular modeling simulations and thermodynamic approaches to investigate compatibility/incompatibility of poly(L-lactide) and poly(vinyl alcohol) blends. *ScienceDirect* **2006**, 47, 8061–8071.
- [22] Y. Lam, G. Goldbeck-Wood, *Polymer* **2003**, 44, 3593.
- [23] A. Chen, X. Peng, K. Kallum, B. Miller, Superhydrophobic tin oxide nanoflowers. *Chem. Commun.* **2004**, 1964–1965.
- [24] S. P. Pottle, Novel mathematical description of surfactants macroaggregates. *Colloids Surf. A* **2001**, 177(1), 13–21.
- [25] M. Lazzari, personal communication, **2008**.